A Plasmonic Nanosensor for Immunoassay *via* Enzyme-Triggered Click Chemistry

Yunlei Xianyu,[†,‡] Zhuo Wang,[†] and Xingyu Jiang[*,†]

[†]Beijing Engineering Research Center for BioNanotechnology & Key Laboratory for Biological Effects of Nanomaterials and Nanosafety, National Center for NanoScience and Technology, Beijing 100190, China and [‡]University of Chinese Academy of Sciences, Beijing 100049, China

ABSTRACT Current techniques for plasmonic immunoassay often require the introduction and additional conjugation of enzyme, and thus cannot accommodate conventional immunoassay platforms. Herein, we develop a plasmonic nanosensor that well accommodates conventional immunoassays and dramatically improves their sensitivity and stability. This plasmonic nanosensor directly employs alkaline phosphatase-triggered click chemistry between azide/alkyne functionalized gold nanoparticles as the readout. This straightforward approach broadens the applicability of nanoparticle-based immunoassays and has great potential for applications in resource-constrained settings.

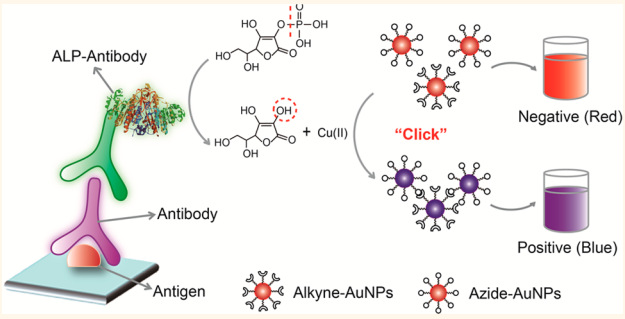

KEYWORDS: plasmonic immunoassay · alkaline phosphatase · click chemistry · gold nanoparticles · naked-eye readout

Advances in nanotechnology endow nanoscale materials as promising candidates for developing plasmonic sensors.[1−4] Gold nanoparticles (AuNPs) have drawn particular interest due to their high extinction coefficients and distance-dependent optical properties.[5−7] AuNP-based plasmonic sensors allow the naked-eye readout with simplicity and low cost, which holds great promise for point-of-care detections.[8−10] Enzyme-linked immunosorbent assay (ELISA), which exploits the antigen−antibody recognition and biocatalytic property of an enzyme, is the most widely used format of immunoassay.[11] ELISA has been extensively used in clinical diagnosis, environmental monitoring, and food quality control, as well as laboratory research.[12−14] By means of enzyme-mediated growth or aggregation of AuNPs, researchers have achieved great progress in developing AuNP-based plasmonic sensors for ELISA.[15−17] However, a remarkable issue is that conventional ELISA typically uses either alkaline phosphatase (ALP) or horseradish peroxidases (HRP) as the enzyme for readout, while current studies typically employ other enzymes that could not directly adapt to the conventional ELISA platforms. Consequently, the introduced enzymes have to be additionally conjugated to antibodies or proteins due to the lack of commercially available enzyme conjugates. In addition, the robustness remains troublesome because AuNPs are easily affected by ambient conditions.

The main challenge to develop a plasmonic nanosensor for ELISA is to develop a straightforward strategy that can be directly imposed on the current ELISA platform, meanwhile improving the analytical performances such as sensitivity and robustness. To tackle this issue, we design an enzyme-triggered Cu(I)-catalyzed azide/alkyne cycloaddition (CuAAC) that integrates the signal generation, signal transduction, and signal amplification simultaneously for plasmonic ELISA. CuAAC is the most widely employed reaction within click chemistry and has several extraordinary features as a sensing platform:[18−20] (1) Cu(I) that acts as the catalyst can dramatically enhance the sensitivity; (2) the orthogonal reaction between alkyne- and azide-terminated molecules intrinsically dictates the selectivity; (3) the reaction is robust under ambient conditions (solvent, temperature, pH, and

* Address correspondence to xingyujiang@nanoctr.cn.

Received for review October 14, 2014 and accepted November 21, 2014.

Published online November 21, 2014
10.1021/nn505857g

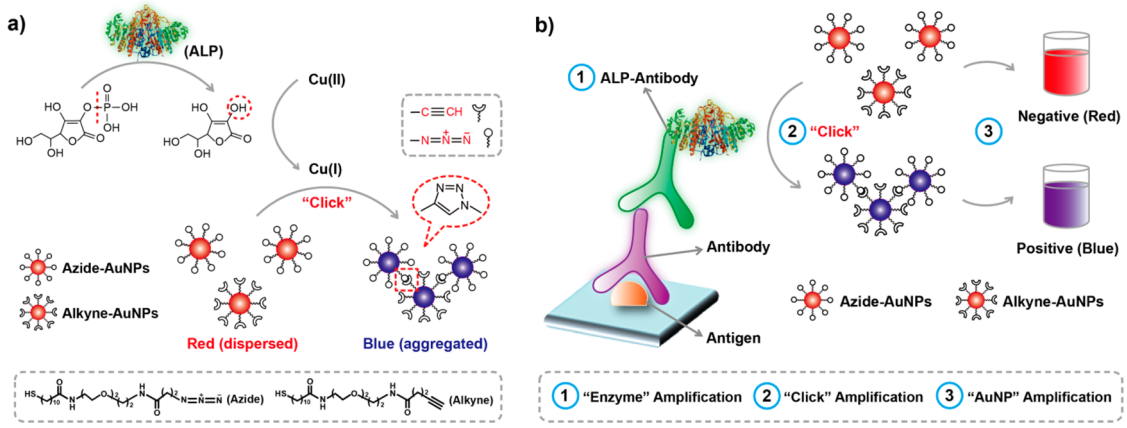

Scheme 1. (a) Plasmonic nanosensor based on ALP-triggered CuAAC between azide- and alkyne-functionalized AuNPs. (b) Naked-eye readout of plasmonic immunoassays based on ALP-triggered CuAAC through three-round amplification.

humidity). These remarkable merits of CuAAC make possible sensors that are remarkable in both sensitivity and selectivity. Our previous work demonstrated that CuAAC can be employed to detect Cu(II) and proteins.[21,22] CuAAC that occurs at the molecular level regulates the aggregation of azide/alkyne-functionalized AuNPs. In this study, we aim to design an enzyme-triggered CuAAC that can be directly exploited for plasmonic nanosensors, considering that ALP and HRP are the two most widely used enzymes (in the form of enzyme-conjugated antibodies) in immunoassays. However, trials with HRP reveal that Cu(I) can inhibit the enzymatic activity of HRP and thus HRP is not suitable for CuAAC-based sensors.[23] This fact leaves ALP as the only possible enzyme for us to develop CuAAC-mediated plasmonic nanosensors that can amplify the signals and enable the naked-eye readout of immunoassays.

ALP is a hydrolytic enzyme that plays a crucial role in the cell signaling pathways. ALP activity has a profound influence on the dephosphorylation process.[24−26] By means of ALP-catalyzed dephosphorylation, we introduce a straightforward signal generation mechanism that triggers CuAAC between alkyne- and azide-functionalized AuNPs (Scheme 1a). In this strategy, ALP enables the removal of a phosphate group from ascorbic acid-phosphate, thus yielding the ascorbic acid as a reductant. Once Cu(II) is transformed into Cu(I) by ascorbic acid, CuAAC occurs between alkyne- and azide-terminated groups, leading to the ALP-triggered aggregation of AuNPs. The overall sensitivity of this plasmonic nanosensor is expected to be high due to the three-round amplification. In the first round, one molecule of ALP could generate many molecules of ascorbic acid through dephosphorylation. The subsequent CuAAC reaction amplifies the detectable signals due to the catalysis of Cu(I), which derives from the reduction of Cu(II) by ascorbic acid. In the third round, AuNPs amplify the CuAAC event to provide a plasmonic readout because of their high extinction coefficient. The "dispersion-to-aggregation" state of AuNPs is displayed with a "red-to-blue" change in color, making possible the naked-eye readout of ALP sensing with high sensitivity.

RESULTS AND DISCUSSION

To implement this concept of a CuAAC-based plasmonic nanosensor for monitoring ALP activity, we first prepared alkyne- and azide-functionalized AuNPs based on ligand-exchange reactions. Bifunctional molecules that contain both alkyne (azide) and thiol groups can modify AuNPs through Au−S bonds. We optimized the bifunctional molecules to improve the reactivity of the alkyne toward the azide, resulting in an enhanced sensitivity and decreased time of CuAAC-based sensor. The reaction is accomplished within 10 min with a limit of detection (LOD) of 1 μM Cu(II). Alkyne- and azide-functionalized AuNPs were prepared in H_2O/*t*BuOH (4:1), and polyethylene glycol-terminated thiols were utilized as the stabilizing agent to prevent proteins from nonspecific adsorption on the AuNPs. The mixture of the two kinds of AuNPs is stably dispersed and exhibits a surface plasmon resonance (SPR) absorption band at 530 nm, which is red (Figure S1, Supporting Information).

The introduction of ALP triggers the CuAAC between alkyne- and azide-functionalized AuNPs, given that both ascorbic acid-phosphate and Cu(II) are present. ALP initiates the generation of the reducing agent (ascorbic acid) that can transform Cu(II) into Cu(I). The signal generation and transduction process result in the aggregation of the AuNPs, which transforms the color of the solution from red to blue, facilitating plasmonic readout with the naked eye. We test the response of ascorbic acid and ascorbic acid-phosphate respectively, to validate the decisive role of ALP in the aggregation of AuNPs. The red color of AuNPs reveals that ascorbic acid-phosphate by itself could not induce the

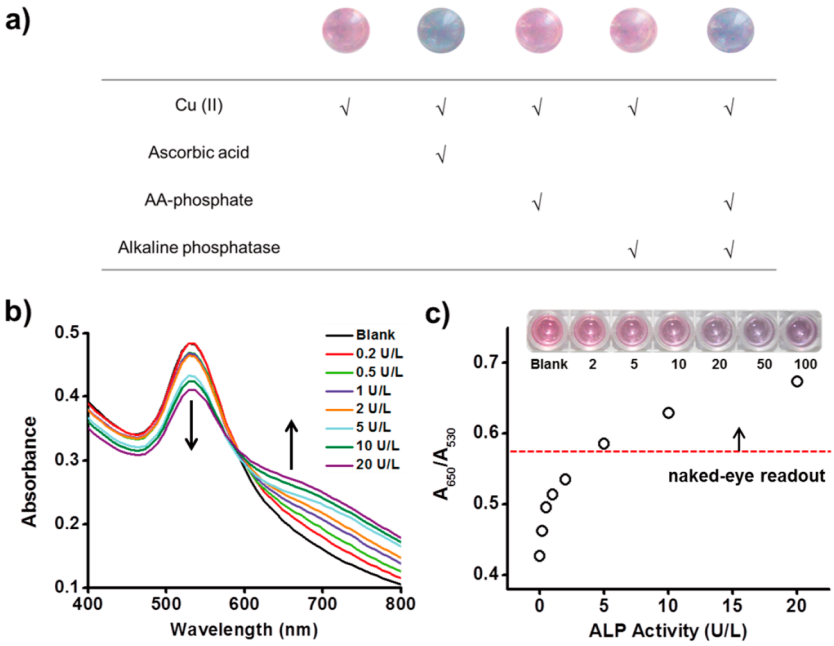

Figure 1. CuAAC-mediated plasmonic nanosensor for ALP sensing: (a) results of adding Cu(II), ascorbic acid (AA), AA−phosphate, and ALP to a mixture of azide- and alkyne-modified AuNPs; (b) UV−vis spectra of the AuNP solution after CuAAC under a range of ALP concentrations; (c) A_{650}/A_{530} value and the corresponding photographs of AuNP solution.

generation of Cu(I) to trigger CuAAC (Figure 1a). ALP alone could not induce a noticeable color change of the AuNP solution either. By contrast, in the presence of ascorbic acid-phosphate, ALP dephosphorylates it to produce ascorbic acid that acts as a reducing agent to generate Cu(I). The subsequent CuAAC reaction leads to the aggregation of AuNPs, turning the solution blue. This obvious change in color provides a convenient and instrument-free means for the readout of ALP sensing.

We test the sensitivity of ALP sensing *via* the color of AuNPs. Final concentrations of ALP ranging from 0.2 U/L to 500 U/L are investigated on the aggregation of AuNPs (Figure S2, Supporting Information). The color of AuNP solution changes from red to blue in this range of concentration. A quantitative characterization of the process by UV−vis spectrometry suggests that the absorbance at 530 nm gradually decreases as the ALP concentration increases (Figure 1b). Meanwhile, the absorbance at 650 nm increases as a consequence of ALP-induced aggregation of AuNPs. We employ the ratio between the absorbance at 650 nm and that at 530 nm (A_{650}/A_{530}) to evaluate the color of the AuNP solution. The A_{650}/A_{530} value increases with the ALP concentration (Figure 1c) and a concentration-dependent color change falls in the range of 5−100 U/L, which enables the naked-eye readout of ALP sensing. The aggregation of AuNPs relates to both the catalysis of ALP and CuAAC, which is a complicated kinetic process, thus the correlation of the A_{650}/A_{530} value to the ALP activity is not linear. The lowest concentration that can be distinguished with a spectrometer

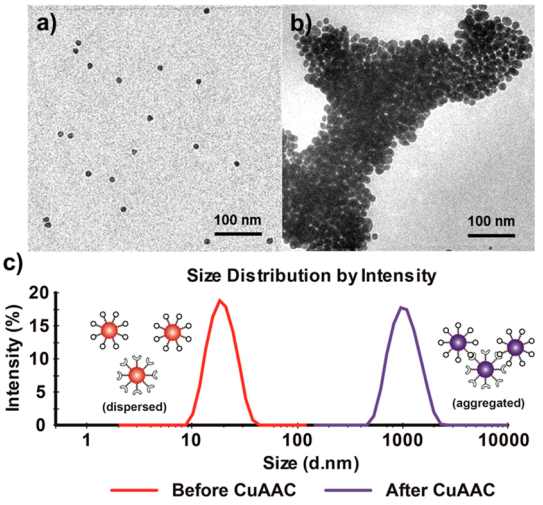

Figure 2. TEM and DLS characterizations of AuNPs: (a and b) TEM images of AuNPs before and after ALP-triggered CuAAC reaction; (c) DLS analysis of AuNPs before and after ALP-triggered CuAAC reaction.

is 0.2 U/L. This sensitivity is considerably higher than previously reported methods that employ AuNPs for the plasmonic sensing of ALP (Table S1, Supporting Information).

To characterize this aggregation process at the nanoscale, we utilize transmission electron microscopy (TEM) to image the AuNPs before and after the ALP-triggered CuAAC. TEM images show that CuAAC reaction results in the aggregation of AuNPs (Figure 2a,b). This aggregation process is also validated by dynamic light scattering (DLS), which indicates that

the hydrodynamic size of AuNPs dramatically enlarges compared to that without ALP (Figure 2c).

We evaluate the specificity of this plasmonic nanosensor for ALP sensing. We test a panel of other proteins and enzymes (bovine serum albumin, human IgG, avidin, HRP, lysosome, and prothrombin) toward this sensor. Among these common types of proteins that one can expect to encounter during an immunoassay in a typical biological application, only ALP can trigger click chemistry-mediated aggregation of AuNPs (Figure S3, Supporting Information). This result matches our expectation considering the excellent specificity of an enzyme (ALP) toward its substrate (ascorbic acid-phosphate). Cu(II) reduction is significant for the plasmonic nanosensor in which Cu(I) acts as a catalyst. Ascorbic acid is the preferred reducing agent because it is convenient and effective during the reaction process. Other reducing agents might not produce Cu(I) considering their different reducing capacities, and they can be washed off to avoid interference in the immunoassays. Another noteworthy point is that Cu(II) may be reduced by proteins in alkaline solutions like the biuret reagent.[22] However, Cu(II) cannot be reduced into Cu(I) by proteins or enzymes in acidic or neutral solutions.[23] In this study, we used Tris-HCl buffer (pH = 7.4) and it would not result in Cu(II) reduction.

We compare the sensitivity and shelf life of this AuNP-based plasmonic sensor with the conventional ALP assay for detection. The principle of conventional ALP assay is based on a color-producing reaction derived from the dephosphorylation of para-nitrophenol phosphate (pNPP) into para-nitrophenol. The lowest concentration of ALP that can be distinguished with the naked eye is 300 U/L for pNPP-based assay, a worse sensitivity than AuNP-based plasmonic sensor (5 U/L) (Figure S4, Supporting Information). Another improvement of our approach is that pNPP must be used immediately after preparation, whereas AuNPs used in our study are stable for an extended period of time. Because of the labile phosphate group of pNPP, it can easily hydrolyze to the colored phenoxide within hours at room temperature. Different from the pNPP-based assay, a remarkable advantage of the CuAAC-mediated approach is the long shelf life of all the reagents required for this plasmonic sensor. The prepared alkyne- and azide-functionalized AuNPs remain stably dispersed even after three months of storage at room temperature (Figure S5, Supporting Information). The good stability is due to both the stabilizing agent (polyethylene glycol-terminated thiol) and the inertness of click chemistry at ambient conditions.

We further employ this plasmonic nanosensor for ELISA that allows naked-eye readout, since enzyme-catalyzed signal transduction and amplification can achieve a high sensitivity.[27−30] We first use the CuAAC-based plasmonic nanosensor to detect a model antibody, rabbit antihuman IgG. In this case, the antigen is human IgG, the primary antibody is rabbit antihuman IgG (target protein), and the secondary antibody is goat antirabbit IgG labeled with ALP. A noteworthy point is that ALP-conjugated antibodies are widely used in the current ELISA platform. Antibody providers such as Abcam, Jackson ImmunoResearch, and Santa Cruz Biotechnology offer a wide range of ALP-labeled antibodies. The procedures of plasmonic ELISA in this study are similar to that of conventional ELISA. After immobilization of these molecules on a 96-well plate, ascorbic acid-phosphate is added to generate ascorbic acid that acts as the reducing agent to produce Cu(I). The CuAAC reaction between alkyne- and azide-functionalized AuNPs leads to the aggregation of AuNPs, thus presenting a visible change in the color of the solution. We test the concentrations of rabbit antihuman IgG ranging from 0.8 ng/mL to 2000 ng/mL. The color of the AuNP solution gradually changes from red to blue as the concentration of target protein increases (Figure 3). The A_{650}/A_{530} value precisely reflects the color and can be employed for the qualitative detection. With a spectrometer, CuAAC-based plasmonic ELISA can detect rabbit antihuman IgG as low as 2 ng/mL (Figure S6, Supporting Information). A control experiment shows that the solution remains red in the absence of rabbit antihuman IgG, suggesting that it is the biospecific recognition of ALP-labeled antibody and target protein that results in the ALP-triggered CuAAC to cause a color change, rather than the nonspecific absorption of ALP-labeled antibody on the well-plate surface.

We compare this type of plasmonic ELISA with conventional ELISA that utilizes pNPP as the substrate. Conventional pNPP-based ELISA relies on distinguishing different shades of the yellow-colored product, resulting in difficulty to discriminate the difference between the solutions with the same color. However, CuAAC-mediated plasmonic ELISA using AuNPs allows a straightforward and naked-eye readout with different colors from a red-colored solution to a blue-colored solution (Figure 3a). CuAAC-mediated plasmonic ELISA allows a naked-eye readout when the concentration of rabbit antihuman IgG is 80 ng/mL (Figure 3b). In comparison, it requires a concentration of 1000 ng/mL in conventional ELISA for the visible readout (Figure 3c). This result represents a 12.5-fold increase in sensitivity for naked-eye detection. The naked-eye detection becomes particularly useful in resource-constrained areas where complex instrumentation such as a plate reader is not available. Therefore, to develop simple and sensitive sensors with naked-eye readout may potentially improve people's living standard in these resource-poor regions.

To test the utility of this approach in real clinical diagnosis, we apply CuAAC-mediated plasmonic ELISA to analyze the serum of patients who suffer from *Mycoplasma pneumonia* (MP) infection. MP is a

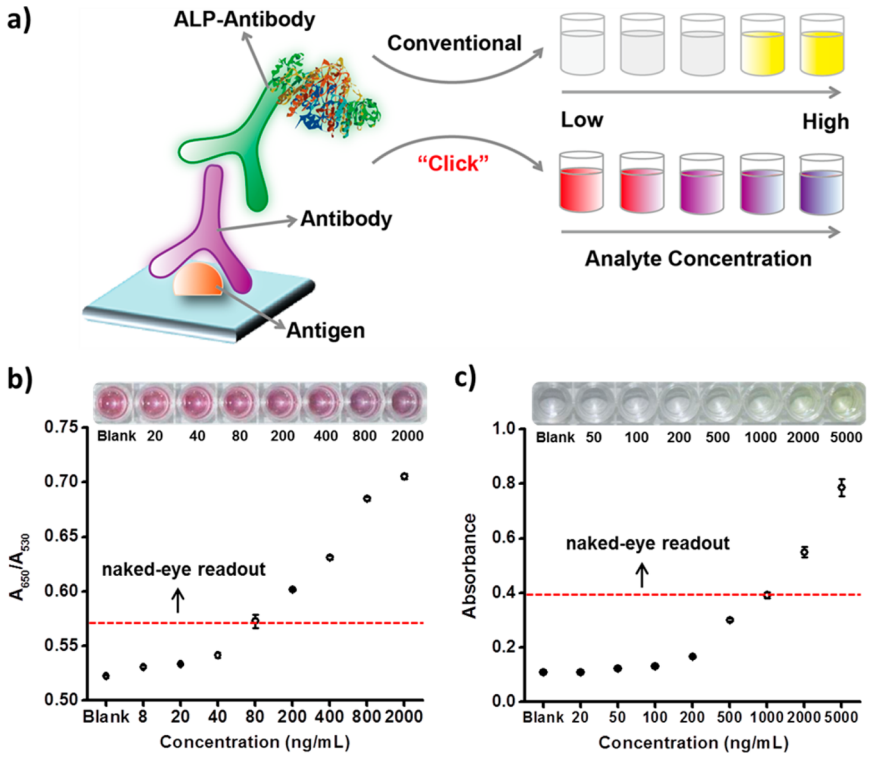

Figure 3. A comparison between CuAAC-mediated plasmonic ELISA and conventional ELISA: (a) schematic illustration of our plasmonic ELISA and conventional ELISA; (b) rabbit antihuman IgG immunoassay based on CuAAC-mediated plasmonic ELISA; (c) rabbit antihuman IgG immunoassay based on conventional ELISA.

"Click" ELISA							
MP antigen	√	√	√	√	√	√	√
BSA	√	√	√	√	√	√	√
Positive serum				P1	P2	P3	P4
Negative serum		N1	N2				
Rabbit anti-human IgM labelled with ALP	√	√	√	√	√	√	√

Figure 4. Human anti-MP IgM immunoassay in real clinical samples using CuAAC-mediated plasmonic ELISA. P1, P2, P3, and P4 indicate different MP-infected patients (positive), while N1 and N2 indicate uninfected (negative).

respiratory pathogen that can be fatal.[31] Serology with IgM is widely recognized for diagnosing the initial infection of MP in clinical practice.[32] Serum from patients that contains anti-MP IgM is diluted to interact with the antigen which is previously immobilized on the 96-well plate. Rabbit antihuman IgM labeled with ALP is subsequently added to recognize human anti-MP IgM. For positive serum samples, this bio-recognition triggers CuAAC between alkyne- and azide-functionalized AuNPs that results in a color change (Figure 4). However, either negative serum samples or blank control remains a red color, showing that CuAAC-mediated plasmonic ELISA has a specific response toward the target analyte. Results from 20 clinical samples (P1 to P20) show that this CuAAC-mediated plasmonic nanosensor enables a naked-eye diagnosis of MP infection (100%), whereas conventional pNPP-based ELISA is not capable of distinguishing with the naked eye in some cases (only 50% can be discriminated) (Figure S7, Supporting Information).

CONCLUSION

We developed a plasmonic nanosensor that employs ALP-triggered CuAAC between azide/alkyne functionalized AuNPs. This plasmonic nanosensor well accommodates current immunoassay platforms and enables naked-eye readout with remarkable enhancement in sensitivity and shelf life. It has great potential for application in on-site detection and resource-poor

settings. We envision enzyme-triggered click chemistry designed in this study to be useful in fields ranging from point-of-care biomedical diagnostics to enzyme-responsive materials.

MATERIALS AND METHODS

Materials. Alkyne-terminated and azide-terminated thiols were provided by Biomatrik Inc. Polyethylene glycol-terminated thiol was purchased from Prochimia. Alkaline phosphatase (ALP) and ascorbic acid-phosphate were purchased from Sigma-Aldrich. Primary antibodies and ALP-conjugated antibodies were purchased from Jackson ImmunoResearch. Anti-Mycoplasma pneumonia (MP) ELISA kit was purchased from EUROIMMUN. All the other reagents/materials required for the experiments were of analytical grade and used as received.

Synthesis of Alkyne/Azide-Terminated AuNPs. AuNPs were prepared by the citrate-mediated reduction of $HAuCl_4$ in aqueous solution. The subsequent ligand exchange reaction was adapted from our previous work. Briefly, the AuNPs were transferred into a solution mixture (H_2O/*t*BuOH = 4:1), followed by the addition of polyethylene glycol-terminated thiol and alkyne-terminated thiol (azide-terminated thiol) dropwise. The ligand exchange reaction was kept at room temperature for 24 h. The sizes of alkyne/azide-functionalized AuNPs (~15 nm) were characterized by DLS (Zeta Sizer Nano ZS, Malvern Instruments Ltd.) and TEM (Tecnai G2 20 S-TWIN, 200 kV).

CuAAC-Mediated ALP Sensing. The alkyne-functionalized AuNPs and azide-functionalized AuNPs were mixed at a volume ratio of 1:1 before use for all the experiments. ALP was serially diluted with 1 mM Tris-HCl buffer to reach a final concentration ranging from 0.2 U/L to 200 U/L in a 96-well plate which contained 20 μL of ALP, 20 μL of ascorbic acid-phosphate (20 mM), and 60 μL of Tris-HCl (1 mM). The solution mixture was kept to react at 37 °C for 1 h. After that, 20 μL of the mixture was added to the well that contained 20 μL of Cu^{2+} (500 μM) and 160 μL of alkyne/azide-AuNPs for the CuAAC reaction. The absorbance of the AuNPs solution was recorded by the plate reader within 10 min.

Plasmonic ELISA for the Model Antibody. For the rabbit antihuman IgG immunoassay, we added 100 μL of human IgG (1.2 μg/mL) in a 96-well plate and incubated the plate at 4 °C overnight. After discarding the solutions, we washed the plate with 0.05% Tween-20 in Tris-HCl buffer and blocked it with 5% bovine serum albumin (150 μL) at 37 °C for 1 h. After that, we washed the wells and added rabbit antihuman IgG of varying concentrations to incubate at 37 °C for 30 min, followed by another washing and addition of goat antirabbit IgG labeled with ALP (0.5 μg/mL). After incubation at 37 °C for 30 min, the wells were washed three times, and 50 μL of ascorbic acid-phosphate (20 mM) was added for a reaction at 37 °C for 1 h. Then 20 μL of solution was taken out for the subsequent CuAAC-based sensing. By contrast, the conventional ALP-based immunoassay differed in that 200 μL of pNPP rather than 50 μL of ascorbic acid-phosphate was directly added in the well and kept to react at 37 °C for 1 h for detection.

Plasmonic ELISA for the Real Clinical Samples. Serum samples from patients who suffered from MP infection were provided by Capital Institute of Pediatrics. For the human anti-MP IgM immunoassay, we employed an anti-MP ELISA kit (EUROIMMUN) that was already coated and blocked for the subsequent experiment. We added diluted human IgM (including real samples, negative control, and blank control) to the wells and incubated them at 37 °C for 30 min. Next, we washed the wells and added 100 μL of rabbit antihuman IgM labeled with ALP (0.5 μg/mL). After incubation at 37 °C for 30 min, the wells were washed three times, and 50 μL of ascorbic acid-phosphate (20 mM) was added for a reaction at 37 °C for 1 h. Then 20 μL of solution was taken out for the plasmonic sensing. The conventional ALP-based immunoassay was carried out for detection as a comparison.

Conflict of Interest: The authors declare no competing financial interest.

Supporting Information Available: Additional results and comparisons with conventional pNPP-based approaches. This material is available free of charge *via* the Internet at http://pubs.acs.org.

Acknowledgment. We thank L. Ma and J. Wang for providing the clinical samples. We also thank X. Zhang, F. Cao, and W. Chen for helpful discussion. We thank the Ministry of Science and Technology of China (2011CB933201), the National Science Foundation of China (21025520, 21105018, 21222502, 91213305), Chinese Academy of Sciences (XDA09030305), and CAS/SAFEA International Partnership Program for Creative Research Teams for financial support.

REFERENCES AND NOTES

1. Xianyu, Y. L.; Jiang, X. Y. Nanoscale Materials and Approaches for Optical Glucose Assays. *Curr. Opin. Chem. Eng.* **2014**, *4*, 144–151.
2. Jans, H.; Huo, Q. Gold Nanoparticle-Enabled Biological and Chemical Detection and Analysis. *Chem. Soc. Rev.* **2012**, *41*, 2849–2866.
3. Du, J. J.; Jiang, L.; Shao, Q.; Liu, X. G.; Marks, R. S.; Ma, J.; Chen, X. D. Colorimetric Detection of Mercury Ions Based on Plasmonic Nanoparticles. *Small* **2013**, *9*, 1467–1481.
4. Zhang, Y.; Guo, Y. M.; Xianyu, Y. L.; Chen, W. W.; Zhao, Y. Y.; Jiang, X. Y. Nanomaterials for Ultrasensitive Protein Detection. *Adv. Mater.* **2013**, *25*, 3802–3819.
5. Du, J. J.; Zhu, B. W.; Peng, X. J.; Chen, X. D. Optical Reading of Contaminants in Aqueous Media Based on Gold Nanoparticles. *Small* **2014**, *10*, 3461–3479.
6. Xianyu, Y. L.; Wang, Z.; Sun, J. S.; Wang, X. F.; Jiang, X. Y. Colorimetric Logic Gates through Molecular Recognition and Plasmonic Nanoparticles. *Small* **2014**, 10.1002/smll.201400479.
7. Wei, J. H.; Zheng, L. T.; Lv, X.; Bi, Y. H.; Chen, W. W.; Zhang, W.; Shi, Y.; Zhao, L.; Sun, X. M.; Li, X. B.; *et al.* Analysis of Influenza Virus Receptor Specificity Using Glycan-Functionalized Gold Nanoparticles. *ACS Nano* **2014**, *8*, 4600–4607.
8. Sun, J. S.; Xianyu, Y. L.; Jiang, X. Y. Point-of-Care Biochemical Assays Using Gold Nanoparticle-Implemented Microfluidics. *Chem. Soc. Rev.* **2014**, *43*, 6239–6253.
9. Luppa, P. B.; Muller, C.; Schlichtiger, A.; Schlebusch, H. Point-of-Care Testing (POCT): Current Techniques and Future Perspectives. *Trends Anal. Chem.* **2011**, *30*, 887–898.
10. Lin, Y. H.; Ren, J. S.; Qu, X. G. Nano-Gold as Artificial Enzymes: Hidden Talents. *Adv. Mater.* **2014**, *26*, 4200–4217.
11. de la Rica, R.; Stevens, M. M. Plasmonic ELISA for the Detection of Analytes at Ultralow Concentrations with the Naked Eye. *Nat. Protoc.* **2013**, *8*, 1759–1764.
12. Chikkaveeraiah, B. V.; Bhirde, A. A.; Morgan, N. Y.; Eden, H. S.; Chen, X. Electrochemical Immunosensors for Detection of Cancer Protein Biomarkers. *ACS Nano* **2012**, *6*, 6546–6561.
13. Liu, D. B.; Huang, X. L.; Wang, Z. T.; Jin, A.; Sun, X. L.; Zhu, L.; Wang, F.; Ma, Y.; Niu, G.; Hight Walker, A. R.; Chen, X. Y. Gold Nanoparticle-Based Activatable Probe for Sensing Ultralow Levels of Prostate-Specific Antigen. *ACS Nano* **2013**, *7*, 5568–5576.
14. Feng, S.; Caire, R.; Cortazar, B.; Turan, M.; Wong, A.; Ozcan, A. Immunochromatographic Diagnostic Test Analysis Using Google Glass. *ACS Nano* **2014**, *8*, 3069–3079.
15. de la Rica, R.; Stevens, M. M. Plasmonic ELISA for the Ultrasensitive Detection of Disease Biomarkers with the Naked Eye. *Nat. Nanotechnol.* **2012**, *7*, 821–824.
16. Liu, D. B.; Wang, Z. T.; Jin, A.; Huang, X. L.; Sun, X. L.; Wang, F.; Yan, Q.; Ge, S. X.; Xia, N. S.; Niu, G.; Liu, G.; Walker, A. R. H.; Chen, X. Y. Acetylcholinesterase-Catalyzed Hydrolysis Allows Ultrasensitive Detection of Pathogens with the

Naked Eye. *Angew. Chem., Int. Ed.* **2013**, *52*, 14065–14069.
17. Nie, X. M.; Huang, R.; Dong, C. X.; Tang, L. J.; Gui, R.; Jiang, J. H. Plasmonic ELISA for the Ultrasensitive Detection of Treponema Pallidum. *Biosens. Bioelectron.* **2014**, *58*, 314–319.
18. Li, N. W.; Binder, W. H. Click-Chemistry for Nanoparticle-Modification. *J. Mater. Chem.* **2011**, *21*, 16717–16734.
19. Liang, L. Y.; Astruc, D. The Copper(I)-Catalyzed Alkyne-Azide Cycloaddition (CuAAC) "Click" Reaction and Its Applications: An Overview. *Coordin. Chem. Rev.* **2011**, *255*, 2933–2945.
20. Qu, W. S.; Liu, Y. Y.; Liu, D. B.; Wang, Z.; Jiang, X. Y. Copper-Mediated Amplification Allows Readout of Immunoassays by the Naked Eye. *Angew. Chem., Int. Ed.* **2011**, *50*, 3442–3445.
21. Zhou, Y.; Wang, S. X.; Zhang, K.; Jiang, X. Y. Visual Detection of Copper(II) by Azide- and Alkyne-Functionalized Gold Nanoparticles Using Click Chemistry. *Angew. Chem., Int. Ed.* **2008**, *47*, 7454–7456.
22. Zhu, K.; Zhang, Y.; He, S.; Chen, W. W.; Shen, J. Z.; Wang, Z.; Jiang, X. Y. Quantification of Proteins by Functionalized Gold Nanoparticles Using Click Chemistry. *Anal. Chem.* **2012**, *84*, 4267–4270.
23. Xianyu, Y. L.; Zhu, K.; Chen, W. W.; Wang, X. F.; Zhao, H. M.; Sun, J. S.; Wang, Z.; Jiang, X. Y. Enzymatic Assay for Cu(II) with Horseradish Peroxidase and Its Application in Colorimetric Logic Gate. *Anal. Chem.* **2013**, *85*, 7029–7032.
24. Choi, Y.; Ho, N. H.; Tung, C. H. Sensing Phosphatase Activity by Using Gold Nanoparticles. *Angew. Chem., Int. Ed.* **2007**, *46*, 707–709.
25. Li, C. M.; Zhen, S. J.; Wang, J.; Li, Y. F.; Huang, C. Z. A Gold Nanoparticles-Based Colorimetric Assay for Alkaline Phosphatase Detection with Tunable Dynamic Range. *Biosens. Bioelectron.* **2013**, *43*, 366–371.
26. Li, J. Y.; Gao, Y.; Kuang, Y.; Shi, J. F.; Du, X. W.; Zhou, J.; Wang, H. M.; Yang, Z. M.; Xu, B. Dephosphorylation of D-Peptide Derivatives To Form Biofunctional, Supramolecular Nanofibers/Hydrogels and Their Potential Applications for Intracellular Imaging and Intratumoral Chemotherapy. *J. Am. Chem. Soc.* **2013**, *135*, 9907–9914.
27. Xiang, Y.; Lu, Y. Using Personal Glucose Meters and Functional DNA Sensors To Quantify a Variety of Analytical Targets. *Nat. Chem.* **2011**, *3*, 697–703.
28. Zhou, C. H.; Zhao, J. Y.; Pang, D. W.; Zhang, Z. L. Enzyme-Induced Metallization as a Signal Amplification Strategy for Highly Sensitive Colorimetric Detection of Avian Influenza Virus Particles. *Anal. Chem.* **2014**, *86*, 2752–2759.
29. Wang, X. R.; Hu, J. M.; Zhang, G. Y.; Liu, S. Y. Highly Selective Fluorogenic Multianalyte Biosensors Constructed *via* Enzyme-Catalyzed Coupling and Aggregation-Induced Emission. *J. Am. Chem. Soc.* **2014**, *136*, 9890–9893.
30. Lin, Y. H.; Ren, J. S.; Qu, X. G. Catalytically Active Nanomaterials: A Promising Candidate for Artificial Enzymes. *Acc. Chem. Res.* **2014**, *47*, 1097–1105.
31. Atkinson, T. P.; Balish, M. F.; Waites, K. B. Epidemiology, Clinical Manifestations, Pathogenesis and Laboratory Detection of Mycoplasma Pneumoniae Infections. *FEMS Microbiol. Rev.* **2008**, *32*, 956–973.
32. Beersma, M. F. C.; Dirven, K.; van Dam, A. P.; Templeton, K. E.; Claas, E. C. J.; Goossens, H. Evaluation of 12 Commercial Tests and the Complement Fixation Test for Mycoplasma Pneumoniae-Specific Immunoglobulin G (IgG) and IgM Antibodies, with PCR Used as the "Gold Standard". *J. Clin. Microbiol.* **2005**, *43*, 2277–2285.